J Nanostruct 16(4): 5483-5497, Autumn 2026

RESEARCH PAPER

Electrical and Structural Properties of SnO_2/PANI Nanocomposite for Gas Sensing Applications

Teba Falah AbdulHassan Ajam *, Rusul A. Ghazi

Department of Physics, College of Sciences, University of Babylon, Iraq

ARTICLE INFO

Article History:
Received 02 June 2026
Accepted 12 September 2026
Published 01 October 2026

Keywords:
Cobalt Acetate
H_2S Gas Sensing
Nanocomposite Thin Films
Polyaniline
SnO_2
Spin Coating

ABSTRACT

Plain thin films of pure polyaniline (PANI), tin oxide (SnO_2), PANI/SnO_2 nanocomposite, and cobalt-doped PANI/SnO_2 was prepared by spin-coating. This study systematically characterized the electrical, Hall effect and H_2S gas sensing properties of the synthesized films. The surface was characterized by using XRD, FE-SEM techniques, both of them confirm the prepared surface confirmed the nanocomposite. Electrical conductivity measurements indicated a conductive character in all samples with mid-three order of magnitude at S/cm scale for the whole range. Analysis of the Hall effect indicates that carrier concentration (nH) and Hall coefficient (rHH) values differed significantly, reflecting a change in charge transport mechanism due to composite formation with Co addition. The carrier concentration increased from 9.07×10^{11} cm^{-3} for PANI/SnO_2 to be as large as 1.446×10^{12} cm^{-3} for PANI/SnO_2/Co, indicating that the cobalt species can generate more charge carriers. Gas sensing measurements toward H_2S gas demonstrated significantly improved sensor performance for nanocomposite.

How to cite this article
AbdulHassan Ajam T., A. Ghazi R. Electrical and Structural Properties of SnO_2/PANI Nanocomposite for Gas Sensing Applications. J Nanostruct, 2026; 16(4):5483-5497. DOI: 10.22052/JNS.2026.04.081

INTRODUCTION

Polyaniline (PANI), also known as "aniline black" in the 19th century, has attracted much attention since the 1980s due to its tunable conductivity, low cost, and environmentally friendly nature [1,2]. The main synthesis methods include chemical oxidative, electrochemical, and vapor-phase polymerization, which give specific characteristics to the conductivity and morphology of PANI. The Structural and Property Characteristics of PANI result from its conjugation and presence of dopants that contribute to the increased conductive capability by altering the electronic structure of the material. The Applications of PANI include the utilization of PANI as a sensor material, supercapacitor, water filtration, anti-corrosion coating, and others. However, the disadvantages of PANI include poor sensitivity and selectivity, especially for some gases like H_2S. Therefore, researches pay much attention to nanocompositing with different dopants such as metal oxides and carbon nanotubes [3]. PANI has a high stability, low cost, and facile synthesis procedure.Conducting polymers (CPs) have gained great attention recently as promising material for gas sensor applications because of unique electrical and gas adsorption characteristics [4]. PANI is a polymer with excellent environmental stability and wide conductivity range; therefore, PANI has been utilized for detection of such gases

* *Corresponding Author Email: sci691.teba.falah@student.uobabylon.edu.iq*

as ammonia and nitrogen dioxide. The advantages of CPs in gas sensor applications lie in fast gas reaction rate, solution processability, low power consumption, and flexibility and portability.

Tin oxide (SnO_2) is an n-type semiconductor, as stated in [5]. Thin film SnO_2 demonstrates good prospects for applications in gas sensors and other devices. According to [6,7], metal oxides have good adsorption capabilities and selectivity toward different gas species. SnO_2 is one of the metal oxides widely used in gas sensors because of excellent gas adsorption capability.

PANI/SnO_2 nanocomposites attract special interest for gas sensors because of good electrical characteristics. As described in [8], electrical characteristics are significantly enhanced in composite films. Improved conductivity results from the efficient interactions between polymer chains and tin oxide particles. Moreover, [9] states that the presence of tin oxide particles increases the surface area and gas adsorption capability of the materials. Due to interaction between polymer and metal oxide nanoparticles, gas sensing performance increases. In addition, there is the increase in the number of active sites for gas adsorption due to the presence of tin oxide. According to [10-14], the effective interactions between SnO_2 and polymer leads to enhanced charge transfer through the interface of particles. There is the improvement in interactions and charge transfer within the films due to the inclusion of SnO_2 nanoparticles. Incorporation of metal oxides in the nanocomposite material increases the number of active sites and promotes charge carrier mobility. The strong interactions between the semiconductor nanoparticles and conducting polymer chains improve electrical properties.Recently, cobalt incorporation into conducting polymer nanocomposites has attracted great attention because of significant role in improvement of electrical and gas adsorption properties [15] describes the enhancement of charge carrier transport efficiency due to transition metals incorporation into conducting polymer composites. There is the improvement in sensitivity and sensing capability in addition to the increase in active sites due to the presence of cobalt in the composite films.According to [11], cobalt incorporation promotes interfacial charge transfers and surface activities in nanocomposites. These factors result in higher sensitivity and response rate of sensors due to increased active sites and interaction between metal and gas molecules. In addition, cobalt doping promotes gas adsorption ability of sensors and enhances charge transfer rate. The study mentions that these nanocomposites demonstrate improved interaction with toxic gases and thus improved performance in gas sensing [10] mentions that cobalt-doped semiconductor nanocomposites can be utilized as gas sensor materials for H_2S. In this case, cobalt-doping improves gas sensing performance.

Although many research works have studied the electrical and gas sensing performance of pure PANI and PANI/SnO_2 nanocomposites, there are few works devoted to investigations of cobalt doped thin films. Works such as [9] and [4] have considered only conducting polymer-based gas sensors without any analysis of cobalt acetate incorporation into the PANI/SnO_2 thin films. Most of these papers were concerned with the analysis of single property of the nanocomposites without considering other characteristics. Therefore, more research works are necessary to improve gas adsorption, charge transfer, sensitivity, and room-temperature sensing.

MATERIALS AND METHODS

Materials

Aniline (PANI) served as a conducting polymer whereas tin oxide nanoparticles (SnO_2) were used as the semiconductor metal oxide. Cobalt acetate was applied as the doping material that enhances optical, electrical, and gas sensing properties of the resulting nanocomposites. Hydrochloric acid (HCl) served as the acidic solution during preparation. Distilled water was used for dilutions and cleaning procedures. Glass substrates were used as a support for depositing the nanocomposite thin films.

PANI Solution Preparation

The PANI solution was prepared by dissolving 79 mg of PANI in 100 ml of diluted HCl solution. Diluted hydrochloric acid solution (0.1 M) was prepared from concentrated HCl (12 M) in accordance with the following dilution equation:

$$C1 \times V1 = C2 \times V2$$

It is known that 0.1 ml of concentrated solution is enough to prepare a total volume of 1 liter of 0.1 M diluted HCl solution. Hence, 0.1 ml was taken

to prepare the diluted HCl solution in 100 ml. The prepared solution was stirred using the magnetic stirrer for about 30 minutes at room temperature.

SnO_2 Solution Preparation

The SnO_2 solution was prepared by dissolving 59 mg of SnO_2 nanoparticles in 50 ml of distilled water. The prepared solution was stirred using the magnetic stirrer for about 30 minutes to get homogenous mixture.

PANI/SnO_2 Nanocomposite Solution Preparation

The solution of the PANI/SnO_2 nanocomposite was prepared by combining equal portions (50% each) of PANI and SnO_2 solutions. The combined solution was stirred using the magnetic stirrer for about 30 minutes to achieve uniform distribution of SnO_2 nanoparticles throughout the PANI matrix.

Co-Doped PANI/SnO_2 Nanocomposite Solution Preparation

The cobalt-doped PANI/SnO_2 nanocomposite solution was prepared by dissolving 14.59 mg of cobalt acetate in 100 ml of distilled water at 50°C in presence of the magnetic stirrer. After that, 5 mg of cobalt acetate solution was mixed with 10

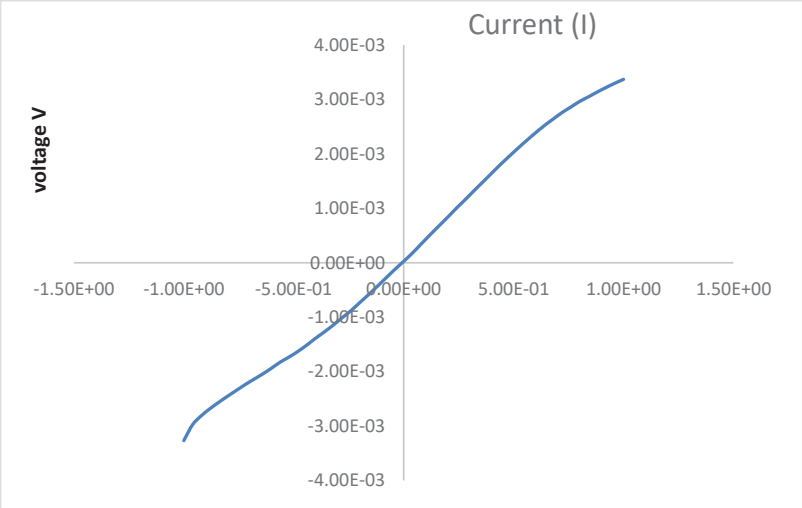

Fig. 1. Current–voltage (I–V) characteristics of the SnO_2 thin film.

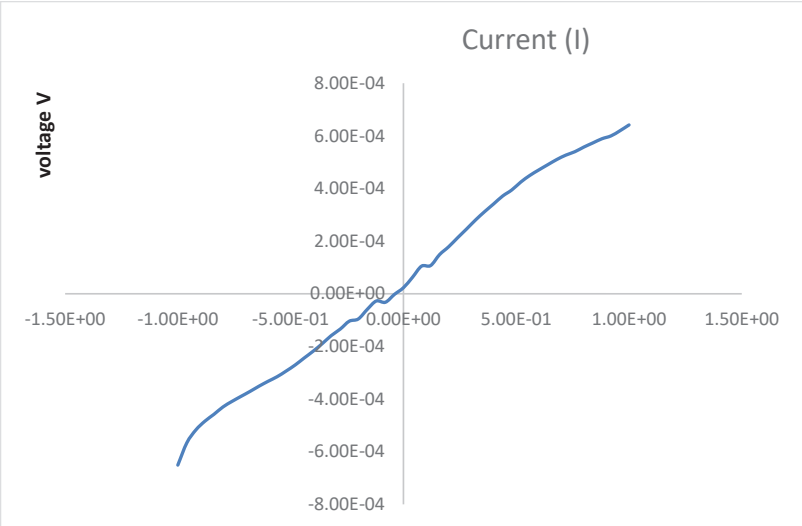

Fig. 2. Current–voltage (I–V) characteristics of the PANI thin film.

ml of PANI/SnO_2 nanocomposite solution and the solution was stirred continuously to obtain homogeneous solution.

Thin Films Deposition by Spin Coating

Deposition of the thin films on cleaned glass substrates was conducted by using spin coating technique. The glass substrates were washed with distilled water and ethanol and then dried before deposition procedure. The prepared solution of PANI/SnO_2 nanocomposites was dropped on a glass substrate mounted on the spin coater apparatus chuck.Spin coating process includes two steps: in the first step, the substrate was rotated at the speed of 500 rpm for 5 seconds and then in the second step – the rotation speed was increased to 2000 rpm for 20 seconds to achieve uniform deposition of the nanocomposite thin film. Thus, the approximate film thickness is 115 nm.

Characterization Techniques

Optical properties of the deposited thin films were determined by UV-Vis spectroscopy using the wavelength range of 180-1200 nm. Electrical properties and H_2S gas sensing performance of the samples were evaluated using special measuring devices in an external laboratory at room temperature conditions.

RESULTS AND DISCUSSION

Electrical properties

The current versus applied voltage (I–V) characteristics of each thin film, PANI, SnO_2, PANI/SnO_2, and PANI/SnO_2/Co show an almost linear relationship confirming a quasi-ohmic conduction in the prepared films. The gradually increase in current with increasing voltage confirms that polymer is Conducting; because the π-electron structure of PANI is conjugated allowing electrons / to show p-type conduction by donating holes in the molecular chain. The doping level controls the electronic properties of these materials as shown in Figs. 1-4.

The pure SnO_2 thin film also exhibited increasing current with voltage applied but maintained a lower level of conductivity than PANI, the orders of magnitude lower conductivity being typical among semiconductor oxide thin films. The introduction of SnO_2 nanoparticles into a PANI matrix resulted in an increase in current response for PANI/SnO_2 nanocomposite, as well as enhanced conductivity relative to pure SnO_2 until 1.0 wt.% of the SnO_2 nanoparticles, which enabled simplified sensor detection and hastened charge

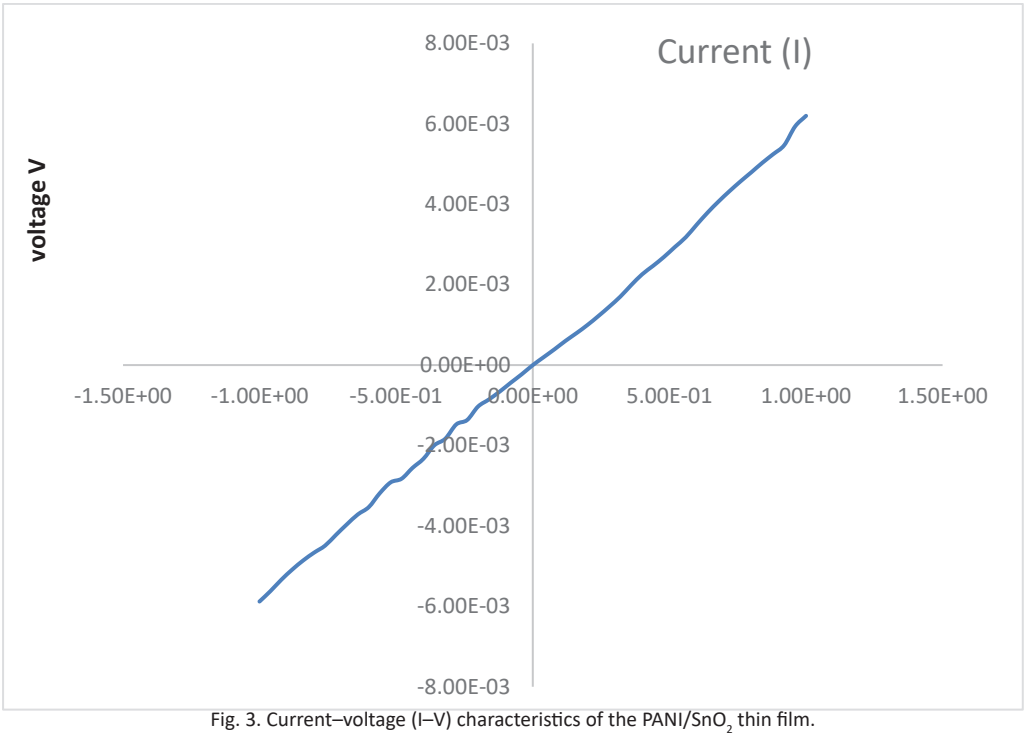

Fig. 3. Current–voltage (I–V) characteristics of the PANI/SnO_2 thin film.

transfer transmission within the composites. The improvement could be related to enhanced interfacial contact between PANI chains and SnO_2 nanoparticles, along with facilitated charge transfer pathways within the nanocomposite structure.In one study, the addition of SnO_2 nanoparticles in the conducting polymer matrix improved electrical conductivity of prepared nanocomposites and showed similar electrical behaviour, also as found in studies like [16], and [17].Moreover, even after the incorporation of cobalt acetate into PANI/SnO_2 nanocomposite, the synthesized thin film still demonstrated conductive nature with moderately high conductivity values. It is possibly attributed to the creation of more pathways for charge transport, increased facilitation of interfacial polarization and defect-related charge carriers contributed from the cobalt species within the nanocomposite films.

In general, the measured electrical behaviour corroborates that PANI/SnO_2 and PANI/SnO_2/Co nanocomposites can enhance charge transfer processes in comparison with pure materials. These findings are also in agreement with previous studies which suggested that PANI-type nanocomposites offer enhanced electrical conductivity, improved sensing responses, and charge carrier mobility.

The electrical conductivity of the thin films is calculated and listed in Table 1. The pure PANI

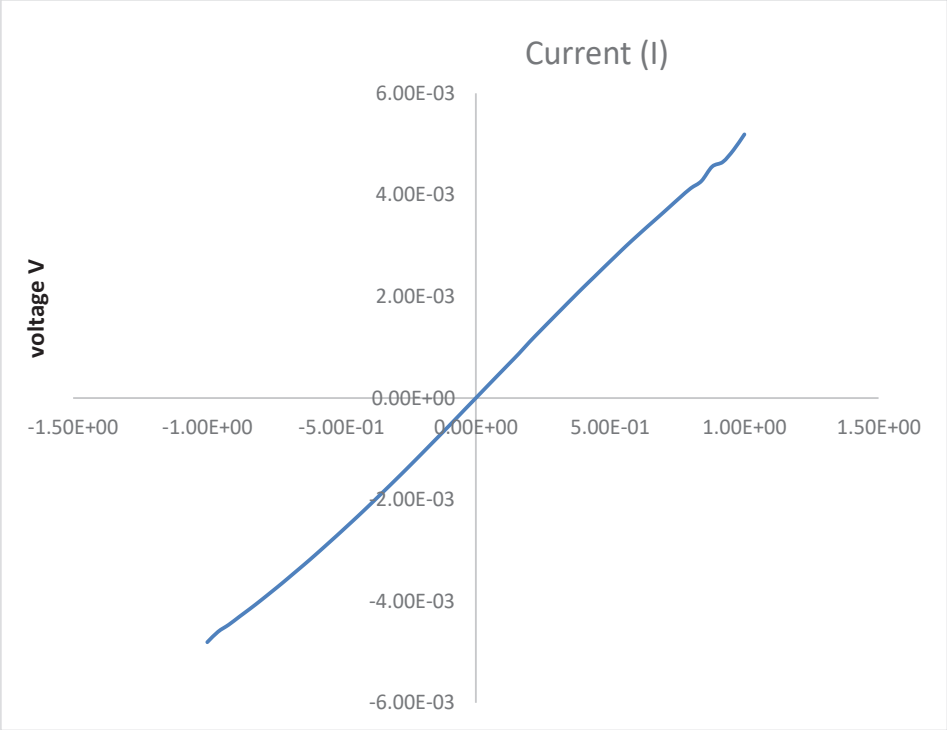

Fig. 4. Current–voltage (I–V) characteristics of the PANI/SnO_2/CO thin film.

Table 1. Calculated electrical conductivity (σ) values of the prepared thin films.

Sample	Slope	σ S/cm
SnO_2	3.42×10^{-3}	8.55×10^{-4}
PANI	6.39×10^{-4}	1.597×10^{-3}
PANI /SnO_2	5.86×10^{-3}	1.46×10^{-3}
PANI /SnO_2/CO	5.10×10^{-3}	1.27×10^{-3}

thin film showed a value of electrical conductivity 1.597×10^{-3} S/cm, which can be observed with the conducting nature of polyaniline polymer chains as well as high mobility charge carriers during conduction due to π-electron system between atoms in molecules having conjugated bonds. In comparison, pure SnO_2 showed the lowest conductivity value (8.55×10^{-4} S/cm), which corresponds to the semiconducting behavior of metal oxide thin films.The conductivity of the prepared PANI/SnO_2 nanocomposite was determined to be 1.46×10^{-3} S/cm, which is consistent with a great interfacial interaction and charge transfer between the conducting polymer and the semiconductor nanoparticles, allowing good electrical conduction to be still present. A similar behavior was available in [18,19] which indicated that the electrical performance of SnO_2 nanoparticles reinforced PANI-based nanocomposites were enhanced.

In addition, the conductivity of PANI/SnO_2/Co nanocomposite was equal to 1.27×10^{-3} S/cm. The film was still electrically conductive albeit at a slightly lower level than pure PANI. This behavior should be associated with cobalt acetate influence on charge transport mechanisms, interfacial polarization, and defect-related charge carriers in the nanocomposite structure. The results secured demonstrated that all fabricated nanocomposite films have adequate electrical conductivity for sensor and optoelectronic applications.

The Hall coefficient (RH) and carrier concentration (nH) of various PANI, SnO_2, PANI/SnO_2 and Co-doped-PANI/SnO_2 thin films are listed in Table 2. It has been observed that the electrical transport properties of these films produced using SnO_2 nanoparticles. Furthermore, the relatively high concentration of carriers in pure PANI thin film is due to conducting polymer chains as well as caused by the movement of π-electrons through a conjugated structure. The latter with SnO_2 is a pure form wide band gap semiconductor oxide material, and it exhibited distinct Hall responses.The carrier concentration significantly increased after doping of SnO_2 nanoparticles into PANI matrix and this could be attributed to a stronger charge transfer interaction between semiconductor nanoparticles and conducting polymer chains. In the same manner [20-23], also presented similar behaviour when SnO_2 nanoparticles improved the transport properties of the prepared nanocomposite films. Besides this, the carrier concentration of Co-doped PANI/SnO_2 thin film was determined to be maximum among all prepared samples. The enhanced characteristic may be due to the existence of defect states and improved carrier transport paths inside the nanocomposite structure from the addition of cobalt acetate. The results from the Hall effect confirm that both PANI/SnO_2 and PANI/SnO_2/Co nanocomposites greatly enhance the electrical properties of thin films, demonstrating their potential in electronic and gas sensor applications.

Structure properties

XRD Analysis

Fig. 5 shows the XRD spectra for pure PANI, pure SnO_2, PANI/SnO_2 nanocomposite and Co-doped PANI/SnO_2 thin films which were prepared by spin coating method.

For pure PANI, the XRD pattern shows a broad diffraction peak at low angles (2θ around 20°, indicating that this conducting polymer matrix has a semi-crystalline nature. This kind of conduct is generally associated with a bi-modulus system where ordered, crystalline; domains coexist with amorphous regions along the polymer chains and it is regarded as one of its distinctive features in polyaniline materials. The same situations were noted in [24,25], where PANI was characterized as a semi-crystalline conductive polymer with wide diffraction peaks that results from partial ordering

Table 2. Hall coefficient (RH) and carrier concentration (nH) values of the prepared thin films.

Sample	Hall coefficient (RH)	Charge carrier concentration (nH)
PANI	7.533×10^{8}	8.297×10^{9}
SnO_2	-5.721×10^{4}	-4.905×10^{10}
PANI/SnO_2	6.891×10^{6}	9.07×10^{11}
PANI/SnO_2/CO	4.321×10^{6}	1.446×10^{12}

of polymer chains.

However, the pure SnO_2 sample shows some sharp and strong diffraction peaks, indicating the crystalline phase of tin oxide nanoparticles. All of the diffraction peaks observed is corresponding to tetragonal rutile phase of SnO_2, which matched well with standard crystal data reported for crystalline tin oxide. A similar diffraction behaviour was observed in [26], stated high-level crystallinity SnO_2 nanoparticles for the sharpness nature of peaks.

For the PANI/SnO_2 nanocomposite, X-ray diffraction pattern revealed concurrent presence of diffraction features corresponding to both phases (PANI and SnO_2) confirming that SnO_2 nanoparticles have been successfully attained into polymer matrix without formation of unwanted secondary phases. In addition, small changes in peak intensity and broadening can suggest interfacial interaction of the conducting polymer chains with semiconductor nanoparticles. That is the major origin of great interfacial interactions between PANI and SnO_2, which can enhance charge transfer properties as well as functional performance as evidenced by previously studies on other kinds of conductive polymer/SnO_2 nanocomposites.

With the addition of cobalt, the diffraction peaks of PANI/SnO_2/Co nanocomposite still demonstrate some additional changes in intensity and broadening behavior, indicating that added species such as cobalt play an active role in overhauling how a crystalline material is arranged and the State of Stress (SOS) with defect types. These types of structural changes may lead to increased active sites, enhanced charge transport and better surface activity which further facilitate sensing applications. Similar findings describing the effect of Co on SnO_2 nanostructures regarding crystallinity and defect density have been reported in [24].

The XRD showed a clear structural change between the prepared PANI, SnO_2, PANI/SnO_2 and PANI/SnO_2/Co thin films (Tables 3-6). p-PANI showed a diffraction peak at 2θ = 11.456°, 20.456° and another peak at 21.087° with an average size of crystallite of about 135.466 nm geopolymer The peaks reflect the presence of an ordered region in conjunction with amorphous regions in the polymer structure, indicating that PANI is semi-crystalline. A semi-crystalline structure of PANI, like that reported in the studies "Electrochemical Synthesis of Polyaniline and Sheet-like $MoSe_2$/PANI Composite for Supercapacitor Applications" and "Morphological and Structural Analysis of Polyaniline and Poly(o-anisidine) Layers Generated in a DC Glow Discharge Plasma by Using an Oblique Angle Electrode Deposition Configuration," was

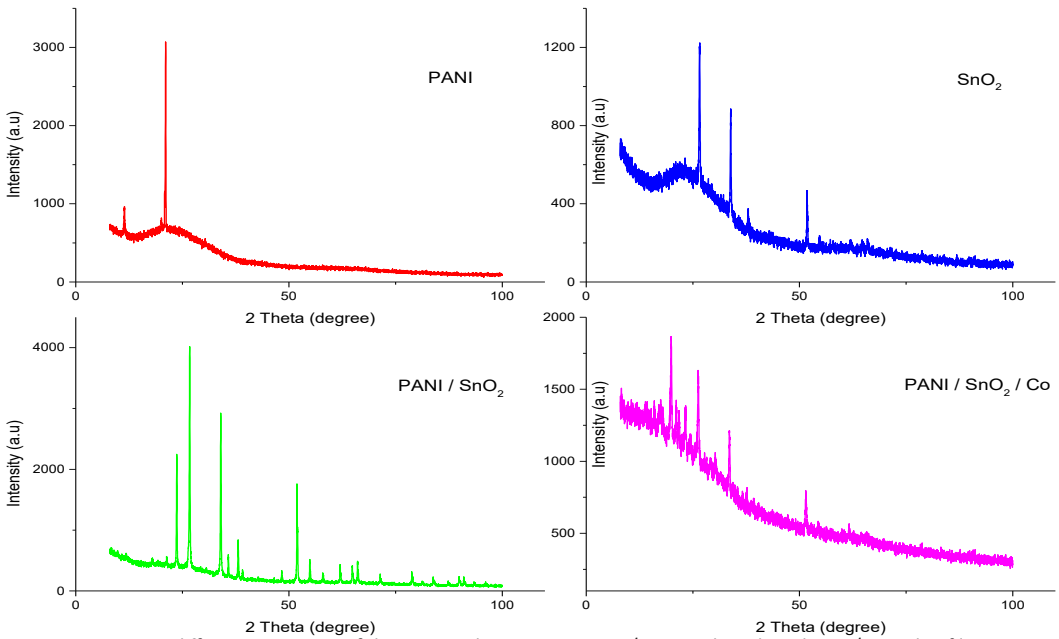

Fig. 5. X-ray diffraction patterns of the prepared PANI, SnO_2, PANI/SnO_2 and Co-doped PANI/SnO_2 thin films.

found due to the crystalline domains dispersed within an amorphous polymer matrix as attributed from the diffraction patterns of PANI.

The measured XRD of the pure SnO_2 thin film as illustrated in Fig. 5 shows diffraction peaks at 2θ = 26.582°, 33.871°, 37.943°, 51.891° and 54.736° representing (110), (101), (200), (211) and (220) crystallographic planes respectively. These peaks confirm the tetragonal rutile SnO_2 phase formation, which is in accordance with reference card 96-900-9083. The crystallite size of pure SnO_2 had an average size of ≈98.0 nm. Similar tetragonal rutile structures and diffraction planes of SnO_2 have been in [8,7]. The peaks which observed at 21.766°–51.500° were due to the incorporation of SnO_2 nanoparticles into PANI, indicating that certain crystallinity was retained in the composite prepared by using the PANI/SnO_2 nanocomposite. Peaks corresponding to both the polymer and SnO_2 are observed, showing that the nanocomposite is correctly formed. The average crystallite size also decreased to 32.828 nm compared with pure PANI and pure SnO_2. This decrease would be related to the limitation of SnO_2 crystal growth led by surrounding PANI chains and the strong interfacial interaction between conducting polymers and semiconductor nanoparticles. Similar behavior was reported in [278,] where the incorporation of SnO_2 into the PANI matrix resulted in the coexistence of diffraction peaks from both phases and modification of crystallite size and structural properties of the nanocomposite. The lower crystallite sizes of the PANI/SnO_2 nanocomposite may yield more grain boundaries and expose surface sites. These structural features are favorable for gas sensitive, because they can improve the adsorption of gases and enhance the interaction between target molecules and sensing surface. Similar observations have been reported in [2,21], where the increase in surface area and active sites resulting from smaller crystallite sizes improved gas adsorption and sensing

Table 3. XRD structural parameters of PANI thin film obtained from XRD analysis.

No.	2θ (°)	d (Å)	FWHM (°)	Crystallite size (nm)
1	11.456	7.724	0.065	140.1
2	20.456	4.428	0.054	175.5
3	21.087	4.213	0.097	90.8
Average	—	5.455	0.072	135.466

Crystal system: Tetragonal (rutile)
Lattice parameters: a = b = 4.737 Å, c = 3.186 Å, Reference code: 96-900-9083.

Table 4. XRD structural parameters of SnO_2 thin film obtained from XRD analysis.

No.	2θ (°)	d (Å)	FWHM (°)	Crystallite size (nm)	(hkl)
1	26.582	3.358	0.065	143.2	(110)
2	33.871	2.646	0.054	180.5	(101)
3	37.943	2.371	0.173	50.9	(200)
4	51.891	1.765	0.130	72.4	(211)
5	54.736	1.677	0.216	43.0	(220)
Average	—	2.363	0.127	98.0	—

Table 5. XRD structural parameters of PANI/ SnO_2 thin film obtained from XRD analysis.

No.	2θ (°)	d (Å)	FWHM (°)	Crystallite size (nm)
1	21.766	4.083	0.216	38.9
2	23.349	3.817	0.260	32.2
3	26.230	3.397	0.173	49.4
4	30.293	2.950	0.520	16.1
5	33.586	2.668	0.216	39.9
6	37.657	2.388	0.346	24.8
7	51.500	1.773	0.317	28.5
Average	—	3.010	0.292	32.828

performance.

Introducing cobalt acetate modifications in the XRD parameters of PANI/SnO_2/Co thin film were made. Diffraction peaks at 2θ values of between 21.309° and 61.974°. In addition, the average FWHM and crystallite size are respectively 0.134° and 83.062 nm. Compared with the undoped PANI/SnO_2 nanocomposite, cobalt incorporation increased the average crystallite size from 32.828 nm to 83.062 nm and altered some of the peak positions and widths. This observation suggests that cobalt acetate affected both the nucleation and growth behavior of crystalline domains in addition to structural reorganization within the nanocomposite. Similar behavior has been discussed in [11,24] where cobalt incorporation modified crystallinity, defect concentration, and surface activity in SnO_2-based materials.

The alterations in the PANI/SnO_2/Co diffraction pattern could thus be reasonably identified for structural modification and defects induced by cobalt. Similar cobalt-induced structural modifications and defect generation have also been reported [24].

To sum up, the XRD results prove that the addition of SnO_2 nanoparticles and cobalt acetate plays an important role in the structural parameters of obtained thin films. The maximum average crystallite size was observed in Pure PANI (135.466 nm) which then followed by pure SnO_2 (98.0 nm). Highest crystallite reduced size (32.828 nm) was observed for the PANI/SnO_2 nanocomposite, and it can be due to stronger interfacial interactions between polymer matrix and SnO_2 nanoparticles. Similar behavior was reported in [8,27] where the incorporation of SnO_2 nanoparticles into the PANI matrix modified the crystallite size and structural characteristics of the prepared nanocomposites.

Cobalt acetate subsequently increased the mean crystallite size to 83.062 nm, and changed positions and widths of the diffraction peaks profiles. Similar observations were reported in [11,24] where cobalt incorporation altered crystallinity, defect concentration, and diffraction

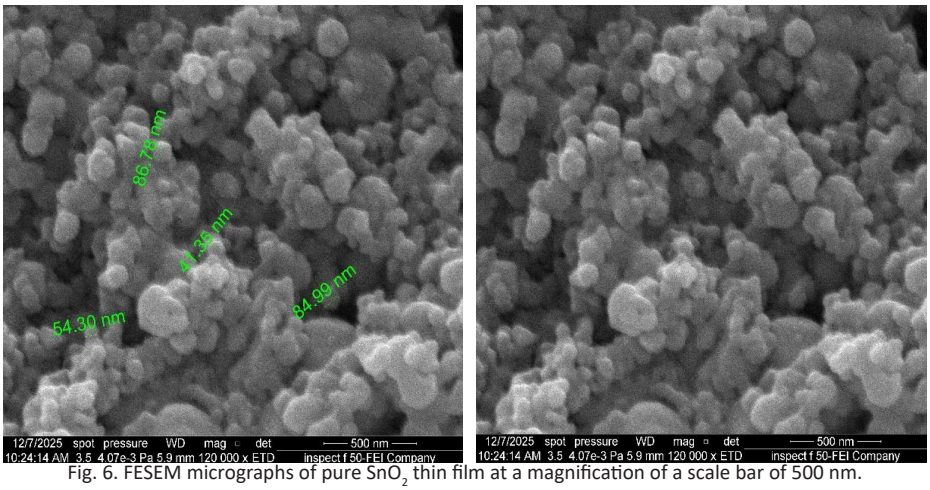

Fig. 6. FESEM micrographs of pure SnO_2 thin film at a magnification of a scale bar of 500 nm.

Table 6. XRD structural parameters of PANI/ SnO_2/CO thin film obtained from XRD analysis.

No.	2θ (°)	d (Å)	FWHM (°)	Crystallite size (nm)
1	21.309	4.169	0.108	80.8
2	23.672	3.758	0.076	114.4
3	26.692	3.339	0.152	56.7
4	33.990	2.634	0.150	58.5
5	38.065	2.362	0.106	85.8
6	51.885	1.760	0.119	79.5
7	54.867	1.761	0.107	90.4
8	61.974	1.496	0.104	93.6
Average	—	—	0.134	83.062

behavior in SnO_2-based materials.The structural modifications are likely to impact the optical absorption, electrical charge transport and surface place and gas sensing functionality of the fabricated nanocomposite thin films. Similar relationships between structural modification and enhancement in optical, electrical and sensing properties have been discussed in [14,].

FESEM

FESEM shows some relevant modifications on the surface morphology of prepared thin films once SnO_2 nanoparticles and cobalt acetate were added (Figs. 6 and 7).

FESEM images of pure SnO_2 thin film (Fig. 6) revealed dense agglomerated nanoparticles with almost spherical shape and average particle size of approximately 88.64 nm. Because of their high surface energy and significant interparticle affiliation, the agglomeration can be frequently observed in metal oxide nanoparticles; therefore, a different approach has been used to eliminate this agglomeration. The reason for that is the morphology of SnO_2 nanostructures which gives us a suitable large surface area in order to optimize adsorption processes and maximize sensing performance. Similar agglomerated and nearly spherical morphologies of SnO_2 nanoparticles have been reported in [28-30], where nanoparticle aggregation was attributed to the high surface energy and strong interaction between neighboring particles.

Fig. 7 shows the further morphological changes in PANI/SnO_2 system after addition of cobalt acetate. PANI/SnO_2/Co nanocomposite revealed the presence of larger agglomerated particles as well as cluster-like structures with an average particle size of approximately 115.12 nm, which is higher than that of PANI/SnO_2 undoped nanocomposite. The change in particle size may be due to a cobalt-induced nucleation and coalescence of the thin film. In addition, species of cobalt may facilitate the clumping up of particles whilst also altering the surface energy of the nanocomposite, leading to increased grain size and extra active sites. Similar effects of cobalt incorporation on particle growth, agglomeration, and surface defect formation have been reported in [31,32], where cobalt doping modified the morphology of SnO_2-based materials and increased the number of active surface sites responsible for enhanced sensing performance.

In conclusion, the FESEM analysis showed that SnO_2 nanoparticles reduced particle size from 92.95 nm for pure PANI to 75.71 nm (PANI/SnO_2 nanocomposite) while the presence of cobalt increased particle size due to its aggregation effect up to 115.12 nm. It is anticipated that these morphological alterations will significantly impact charge transport, gas adsorption ability, and finally the H_2S gas sensing performance of the resulting thin films. Similar observations regarding the reduction of particle size after incorporation of SnO_2 nanoparticles into PANI matrices were reported in [31,32]. Furthermore, the increase in particle size and aggregation behavior after cobalt incorporation were found to be consistent with the results reported in [11,24].

The FESEM results showed that the average

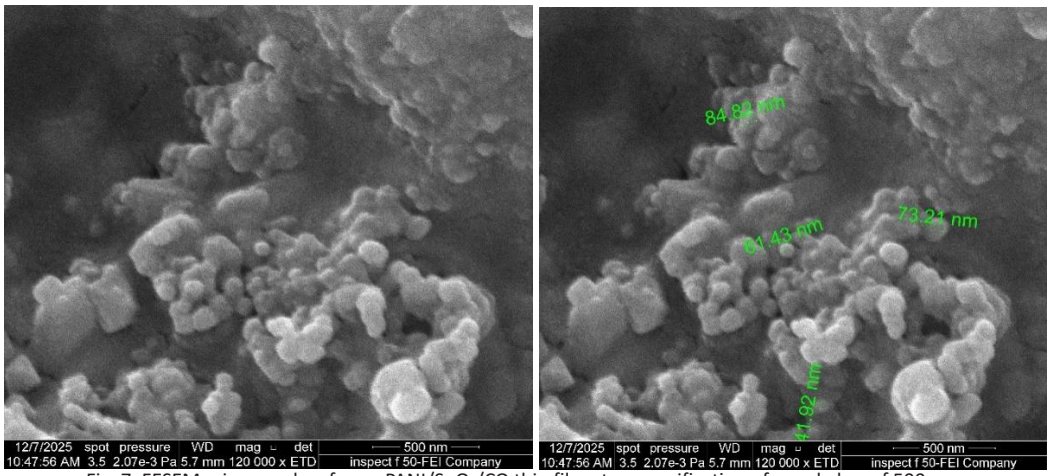

Fig. 7. FESEM micrographs of pure PANI/SnO_2/CO thin film at a magnification of a scale bar of 500 nm.

particle size decreased from 92.95 nm for pure PANI and 88.64 nm for pure SnO_2 to 75.71 nm for the PANI/SnO_2 nanocomposite, indicating improved nanoparticle dispersion and stronger interfacial interaction between PANI and SnO_2. However, the addition of cobalt increased the particle size to 115.12 nm due to particle agglomeration and grain growth effects. Similar observations have been reported in [32,24].

Gas Sensing

Figs. 8-11 illustrates the gas sensing response of pure PANI, pure SnO_2, PANI/SnO_2 and PANI/SnO_2/Co thin films for H2S gas versus time. The approach allowed monitoring of the variation of electrical resistance during exposure to H_2S gas followed by recovery in air, where all gas sensing measurements were performed at room temperature. They showed that all of the prepared samples were responsive to H_2S gas but with different sensing behaviors, which depend on composition and surface characteristics for nanosheets at least up to 5.

Upon exposure to H_2S gas, the resistance of

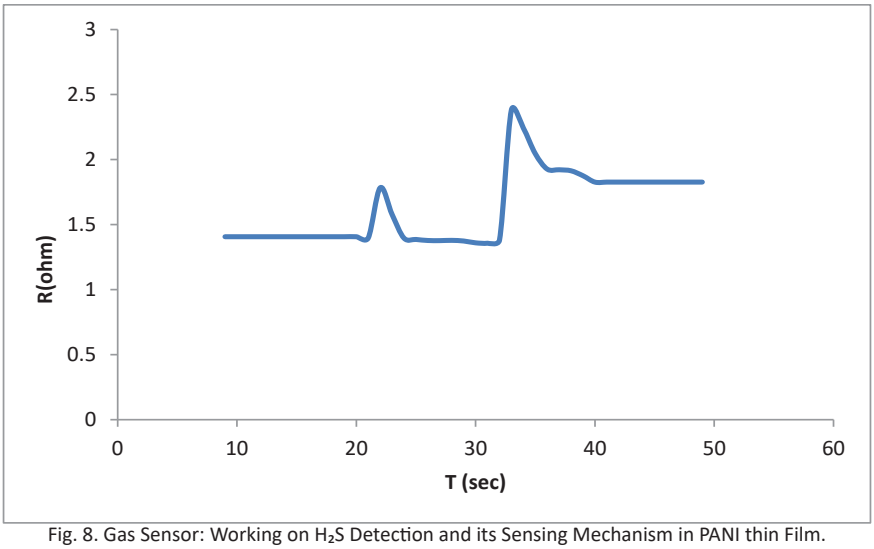

Fig. 8. Gas Sensor: Working on H_2S Detection and its Sensing Mechanism in PANI thin Film.

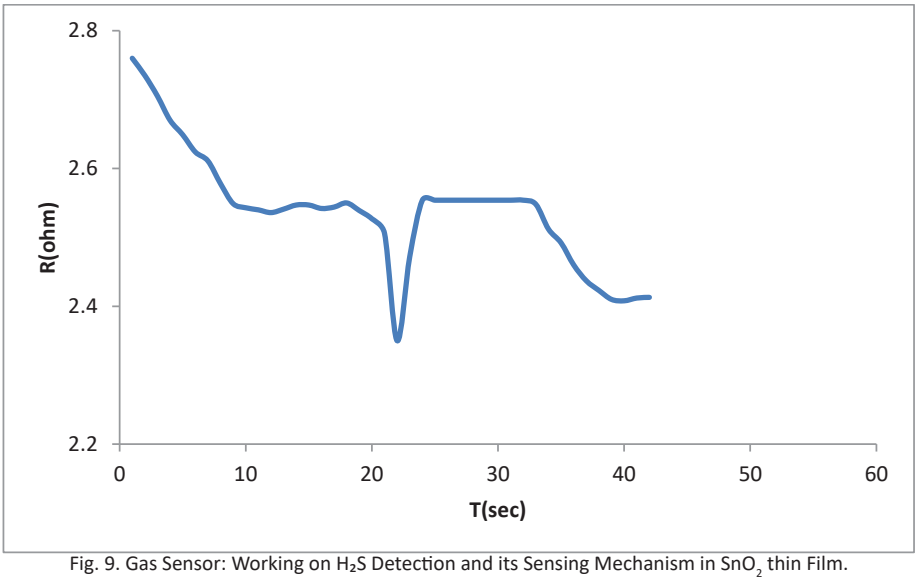

Fig. 9. Gas Sensor: Working on H_2S Detection and its Sensing Mechanism in SnO_2 thin Film.

pure PANI sample was sharply increased, which is assumed to be due to the interaction between gas molecules and conductive polymer chains. Polyaniline exhibits good sensitivity to toxic gases owing to the gas–polymer chain interaction, whereby the electrical conductivity of the material varies with gas adsorption [17]. Additionally, [18] mentioned that the PANI sensing mechanism emerges from the interaction between gas molecules and PANI, which modifies the electrical conductivity and causes a change in charge carrier concentration due to adsorption. The improved resistance observed in the present work also corroborates the favorable interaction of H_2S molecules with the conjugated polymer matrix.

However, pure SnO_2 sample showed a reverse trend as all other samples and the resistance was decreased during exposure to H_2S gas. That behaves like n- type semiconductor material (e. g., SnO_2) They found that when n-type

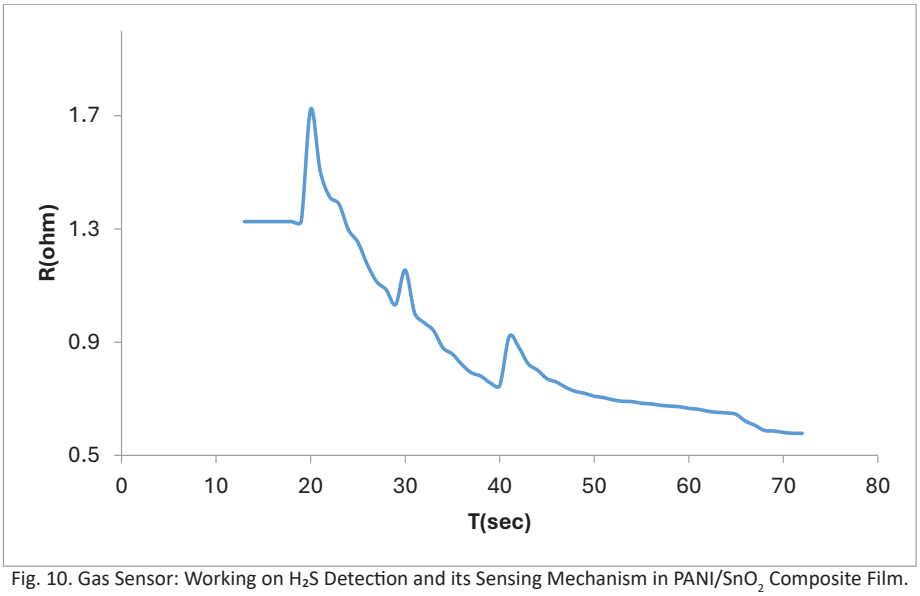

Fig. 10. Gas Sensor: Working on H_2S Detection and its Sensing Mechanism in PANI/SnO_2 Composite Film.

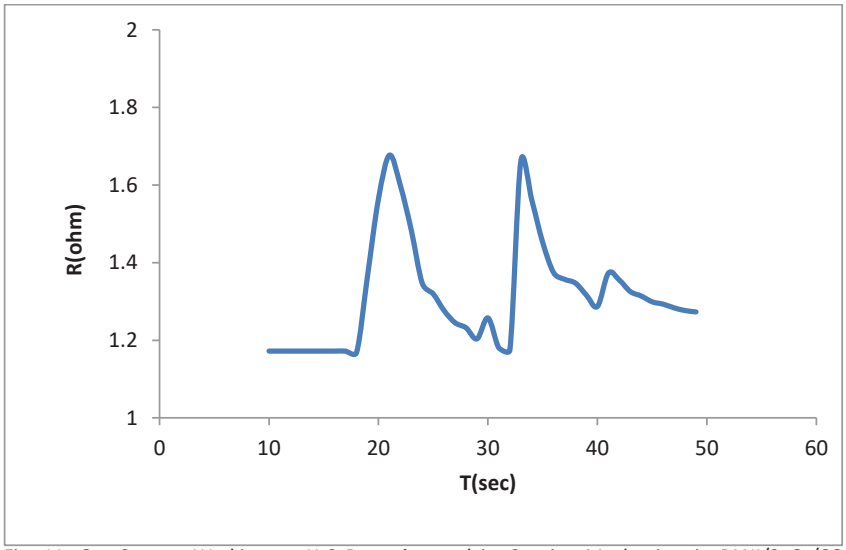

Fig. 11. Gas Sensor: Working on H_2S Detection and its Sensing Mechanism in PANI/SnO_2/CO Composite Film.

semiconductors were exposed to reducing gases like H_2S, electrons are released into the conduction band and electrical resistance is lowered [5]. SnO_2 is an n-type semiconductor and because electrons are donating processes involving reducing gasses, the resistance drops. Moreover, [21] adsorbing oxygen species on the surface of SnO_2 interact with reducing gases and release captured electrons, leading to a decrease in the resistance. So, the different between p-type conducting polymers and n-type metal oxide semiconductors type are proved by reverse sensing behavior of SnO_2 as compared with PANI.

The incorporated SnO_2 nanoparticles into PANI matrix increased active adsorption sites density and facilitated charge transfer during H2S gas exposure, which improved the gas sensing performance. Also, PANI/SnO_2 heterojunction formed the favorable electron transport channel and enhanced the interaction of sensing layer with gas molecules. Similar findings were reported in [15] where the electrical and sensing characteristics of PANI-based nanocomposites improved with the introduction of SnO_2 nanoparticles. Furthermore, [9] and [19] have demonstrated that the synergistic effect of conducting polymers with metal oxide nanoparticles leads to an increase in gas adsorption, sensitivity, and charge transport across the sensing layer. In addition, as was shown in [23], PANI/SnO_2 nanocomposites appear to have increased sensing performance due to a better interfacial interaction between the conducting polymer and semiconductor nanoparticles. Furthermore, the results of this work are in line with previous studies [11], as the PANI/SnO_2 sample showed an improved gas sensitivity response than pure PANI and pure SnO_2 for H_2S detection.

As depicted in Table 7, the PANI/SnO_2/Co sample possessed more H_2S sensitivity than all other prepared samples, which reached a value of about 43.088%. The sensing performance improvement after cobalt acetate addition possibly arises from the surface defects, active adsorption sites, oxygen vacancies and charged transport pathways, as reported in [24].

Cobalt species not only modulate the resistance but also promote adsorption and catalytic dissociation of H_2S molecules on the sensing surface. As reported in [25], cobalt oxide significantly enhances the sensor response toward H_2S through its catalytic activity and improved selectivity. The responses are in good agreement with the results presented previously, confirming that cobalt acetate facilitated gas sensing efficiency of PANI/SnO_2 nanocomposite thin films

Summarizes the various gas sensing characteristics of each prepared thin films, including response time, recovery time, resistance in air (Rair), resistance under H_2S gas atmosphere (Rg), and sensitivity values (Sensitivity = Rg/Rair) are also summarized in Table 7. The results obtained exhibited that the pure SnO_2 thin film had the lowest value of sensitivity (although about 8.255%) and PANI/SnO_2/Co nanocomposite has the highest sensitivity (nearly 43.088%). In contrast, the pure PANI and PANI/SnO_2 showed moderate properties with sensitivity values of approximately 26.723% and 29.939%, respectively.

This difference in sensitivity among the obtained samples could be associated with diversity in sample surface activity and adsorbing capacity, as well as electron transfer processes occurring between sensing films. Furthermore, the response and recovery times suggest that incorporation of SnO_2 nanoparticles and cobalt acetate improved the dynamic sensing performance of prepared NFC thin films .In the studies [23] and [25] reported similar enhancements in gas sensing characteristics of PANI/SnO_2-based

Table 7. Gas sensing characteristics of the prepared thin films.

Sample	T(second) ON	R (Ω) air	T(second) Off	R (Ω) GAS	T(second) RES.	T(second) rec.	H_2S (Sensitivity %)
PANI/SnO_2/CO	18	1.172	21	1.677	3	11	43.088
PANI	20	1.407	22	1.783	4	5	26.723
PANI/SnO_2	17	1.326	20	1.723	4	5	29.939
SnO_2	16	2.544	22	2.35	5	3	8.255

nanocomposites, in which both semiconductor nanoparticles and cobalt species was incorporated to improve the sensitivity with enhanced sensing response towards toxic gases.

Thus, the overall outcomes indicate that PANI/SnO_2/Co thin films exhibit high-performance sensing characteristics at room temperature for H_2S gas detection and are thus candidates for gas sensors.

CONCLUSION

We investigated in this work successful preparation of PANI, SnO_2, PANI/SnO_2 and PANI/SnO_2/Co thin films on glass substrates from spin coating method. Electrical and gas sensing characteristics of the synthesized thin films were studied. The results obtained, established the influence of SnO_2 nanoparticles on the physical properties of prepared films within PANI matrixes. The electrical measurements revealed linear I–V characteristics for all of the samples prepared indicating ohmic conduction behavior. The charge transfer and carrier transport within the polymer matrix facilitated increase of conductivity of the nanocomposite thin films if compared with pure SnO_2. As demonstrated by Hall effect measurements, the prepared films displayed different carrier transport mechanisms depending on film composition.Gas sensing measurements of H_2S gas demonstrated that all prepared samples have gas-sensing activity at room temperature. It was found that, for pure SnO_2 sample the n-type semiconductor response was observed, while all PANI based samples showed a p-type sensing reaction. The improvement in the electronic properties of PANI films coated with SnO_2 nanoparticles was attributed to the improved surface area and active adsorption sites in sensor elements. In addition, the utilization of cobalt acetate appreciably enhanced gas sensing sensitivity as the PANI/SnO_2/Co thin film demonstrates the best sensitivity compared with other prepared samples.The overall obtained results show that the thin films of PANI/SnO_2/Co nanocomposite prepared by spin coating can provide better electrical and gas sensing properties making it a potential material for gas sensing applications.

CONFLICT OF INTEREST

The authors declare that there is no conflict of interests regarding the publication of this manuscript.

REFERENCES

1. Kaushik P, Bharti R, Sharma R, Verma M, Olsson RT, Pandey A. Progress in synthesis and applications of Polyaniline-Coated Nanocomposites: A comprehensive review. Eur Polym J. 2024;221:113574.
2. El-naggar AM, Alsaggaf A, Heiba ZK, Kamal AM, Aldhafiri AM, Fatehmulla A, et al. Exploring the structural, optical and electrical characteristics of PVA/PANi blends. Opt Mater. 2023;139:113771.
3. Kaissner R, Li J, Lu W, Li X, Neubrech F, Wang J, et al. Electrochemically controlled metasurfaces with high-contrast switching at visible frequencies. Science Advances. 2021;7(19).
4. Dong R, Yang M, Zuo Y, Liang L, Xing H, Duan X, et al. Conducting Polymers-Based Gas Sensors: Principles, Materials, and Applications. Sensors. 2025;25(9):2724.
5. Izydorczyk W, Izydorczyk J. Structure, Surface Morphology, Chemical Composition, and Sensing Properties of SnO_2 Thin Films in an Oxidizing Atmosphere. Sensors. 2021;21(17):5741.
6. Bitu MNA, Tanvir NI, Islam S, Farhad SFU. Effect of substrate surface on the wide bandgap SnO_2 thin films grown by spin coating. MRS Advances. 2023;8(5):194-200.
7. Verma A, Shriram K, Das B. Study of structural/microstructural and optical characteristics of tin oxide (SnO_2) thin film grown at different substrate temperatures of 325 °C, 375 °C, 425 °C by spray pyrolysis method. Journal of Optoelectronic and Biomedical Materials. 2025;17(3):141-149.
8. Kumar S, Choudhary RB. Structural, optical, and thermal investigation of SnO_2 nanoparticles incorporated PANI nanofibers as an emissive layer material. J Mol Struct. 2023;1293:136199.
9. Jain A, Dhonde M, Soni A, Kumar A, Sahu K. Polyaniline based blends and composites for gas sensing: A comprehensive review on materials, mechanisms, and applications. React Funct Polym. 2026;220:106610.
10. Liu Z, Liu Y, Zhang L, Poyraz S, Lu N, Kim M, et al. Controlled synthesis of transition metal/conducting polymer nanocomposites. Nanotechnology. 2012;23(33):335603.
11. Basyooni MA, Eker YR, Yilmaz M. Structural, optical, electrical and room temperature gas sensing characterizations of spin coated multilayer cobalt-doped tin oxide thin films. Superlattices Microstruct. 2020;140:106465.
12. Velusamy P, Babu RR, Ramamurthi K, Elangovan E, Viegas J, Sridharan M. Gas sensing and opto-electronic properties of spray deposited cobalt doped CdO thin films. Sensors Actuators B: Chem. 2018;255:871-883.
13. Alharbi N, Siddiq H, Refaei M, Sherly RA, Paulraj R, Florence S. Effects of pH on the synthesis of PANI-Tin oxide nanocomposite as counter electrode in DSSC applications. Journal of Materials Science: Materials in Electronics. 2025;36(13).
14. Bijwe DR, Yawale SS, Kumbharkhane AC, Peng H, Yawale DS, Yawale SP. Complex dielectric behavior of doped polyaniline conducting polymer at microwave frequencies using time domain reflectometry. Revista Mexicana de Física. 2019;65(6 Nov-Dec):590-600.
15. Singh B, Das B, Chauhan VK. Structural, optical and electrical properties of PANI/SnO_2 nanocomposites (Part I – prior polyester blending). The Journal of The Textile Institute. 2022;114(4):692-699.

16. Bagheri-Mohagheghi M-M, Shokooh-Saremi M. The electrical, optical, structural and thermoelectrical characterization of n- and p-type cobalt-doped SnO_2 transparent semiconducting films prepared by spray pyrolysis technique. Physica B: Condensed Matter. 2010;405(19):4205-4210.
17. Fratoddi I, Venditti I, Cametti C, Russo MV. Chemiresistive polyaniline-based gas sensors: A mini review. Sensors Actuators B: Chem. 2015;220:534-548.
18. Bai H, Shi G. Gas Sensors Based on Conducting Polymers. Sensors. 2007;7(3):267-307.
19. Pirsa S. Chemiresistive Gas Sensors Based on Conducting Polymers. Materials Science and Engineering: IGI Global; 2017. p. 543-574. http://dx.doi.org/10.4018/978-1-5225-1798-6.ch022
20. Periyasamy M, Kar A. Modulating the properties of SnO_2 nanocrystals: morphological effects on structural, photoluminescence, photocatalytic, electrochemical and gas sensing properties. Journal of Materials Chemistry C. 2020;8(14):4604-4635.
21. Wang C, Yin L, Zhang L, Xiang D, Gao R. Metal Oxide Gas Sensors: Sensitivity and Influencing Factors. Sensors. 2010;10(3):2088-2106.
22. Kroutil J, Laposa A, Voves J, Davydova M, Nahlik J, Kulha P, et al. Performance Evaluation of Low-Cost Flexible Gas Sensor Array With Nanocomposite Polyaniline Films. IEEE Sens J. 2018;18(9):3759-3766.
23. Han Y, Hao S, Liu L, Li B, Mu Y, Yang M, et al. Fabrication of high-performance NH_3 flexible sensor based on PANI/SnO_2 hollow nanosphere composite. Microchimica Acta. 2025;192(9).
24. Zhang X, Liu B, Xu Y, Liu H, Zhao W, Wang P, et al. Facile fabrication of cobalt-doped SnO_2 for gaseous ethanol detection and the catalytic mechanism of cobalt. CrystEngComm. 2019;21(48):7528-7534.
25. Rumyantseva MN, Vladimirova SA, Vorobyeva NA, Giebelhaus I, Mathur S, Chizhov AS, et al. p-CoO_x/n-SnO_2 nanostructures: New highly selective materials for H2S detection. Sensors Actuators B: Chem. 2018;255:564-571.
26. Khan H, Khan MN, Khan M, Iqbal Y, Ahsan SM, Ullah H. Structural, optical, electrical and photocatalytic properties Ce-doped SnO_2 nanoparticles for photoelectrochemical applications. Journal of Materials Science: Materials in Engineering. 2025;20(1).
27. Anitha R, Kumar E, Rathnakumar K, Vella Durai SC. Synthesis, structural, morphological, optical and electrical studies of PANI / SnO_2 nanocomposites. Journal of Ovonic Research. 2021;17(2):99-106.
28. Beygisangchin M, Abdul Rashid S, Shafie S, Sadrolhosseini AR, Lim HN. Preparations, Properties, and Applications of Polyaniline and Polyaniline Thin Films—A Review. Polymers. 2021;13(12):2003.
29. Kim YJ, Lee HS, Noh J-S. Transient behaviors of ZnO thin films on a transparent, flexible polyethylene terephthalate substrate. Thin Solid Films. 2016;603:160-164.
30. Sagadevan S, Anita Lett J, Alshahateet SF, Fatimah I, Weldegebrieal GK, Le M-V, et al. Photocatalytic degradation of methylene blue dye under direct sunlight irradiation using SnO_2 nanoparticles. Inorg Chem Commun. 2022;141:109547.
31. Vijayalakshmi S, Kumar E, Ganeshbabu M, Venkatesh PS, Rathnakumar K. Structural, electrical, and photocatalytic investigations of PANI/ZnO nanocomposites. Ionics. 2021;27(7):2967-2977.
32. Patil D, Patil V, Patil P. Highly sensitive and selective LPG sensor based on α-Fe_2O_3 nanorods. Sensors Actuators B: Chem. 2011;152(2):299-306.